MELK predicts poor prognosis and promotes metastasis in esophageal squamous cell carcinoma via activating the NF-κB pathway

JIECHENG YE[1,2*], WANYING DENG[1*], YING ZHONG[1], HUI LIU[1], BAOYIN GUO[1], ZIXI QIN[1], PEIWEN LI[1], XUEYUN ZHONG[1] and LIHUI WANG[1]

[1]Department of Pathology, Medical College, Jinan University, Guangzhou, Guangdong 510632; [2]Department of Pathology, The First Affiliated Hospital, Sun Yat-sen University, Guangzhou, Guangdong 510080, P.R. China

Received March 17, 2022; Accepted May 23, 2022

DOI: 10.3892/ijo.2022.5384

Abstract. Esophageal squamous cell carcinoma (ESCC) is one of the most common malignancies worldwide with a low 5-year survival rate due to the lack of effective therapeutic strategies. Accumulating evidence has indicated that maternal embryonic leucine zipper kinase (MELK) is highly expressed in several tumors and associated with tumor development. However, the biological effects of MELK in ESCC remain unknown. In the present study, cell phenotypical experiments and animal metastasis assays were performed to detect the influence of MELK knockdown *in vitro* and *in vivo*. The potential molecular mechanism of MELK-mediated ESCC metastasis was further investigated by western blotting and immunofluorescence staining. The results revealed that the expression of MELK in human ESCC tissues was higher than that in adjacent normal tissues and was positively associated with the poor prognosis of patients. Reducing MELK expression resulted in growth inhibition and suppression of the invasive ability of ESCC cells *in vitro* and *in vivo*. MELK inhibition induced alterations of epithelial-mesenchymal transition-associated proteins. Mechanistically, MELK interacted with IκB kinase (IKK) and promoted the phosphorylation of IKK, by which MELK regulated activation of the NF-κB pathway. Collectively, the present study revealed the function and mechanism of MELK in the cell metastasis of ESCC, which may be a potential therapeutic target for ESCC.

Correspondence to: Professor Lihui Wang, Department of Pathology, Medical College, Jinan University, 601 Huangpu Avenue West, Guangzhou, Guangdong 510632, P.R. China
E-mail: wanglh@jnu.edu.cn

*Contributed equally

Key words: maternal embryonic leucine zipper kinase, esophageal squamous cell carcinoma, tumor metastasis, NF-κB pathway, inhibitor of nuclear factor-κB kinase subunit β

Introduction

Esophageal carcinoma is one of the most common malignancies worldwide with a high mortality rate (1). China accounts for >50% (324,422/604,100) of patients, and 90% of esophageal carcinoma includes esophageal squamous cell carcinoma (ESCC) cases. Although the diagnosis and treatment for ESCC have improved in recent years, the overall 5-year survival rate of patients is 15 to 25% (2-4). The leading cause of treatment failure and mortality among patients with ESCC is tumor recurrence and metastasis (5,6). Tumor metastasis is very complex and involves multiple steps (7); thus, there is an urgent need to discover the underlying molecular mechanisms responsible for ESCC metastasis, as they may serve as targets to improve the treatment of ESCC.

Numerous protein kinases have critical roles in regulating cell growth and survival, and thus, have emerged as the most important targets for drug discovery. Maternal embryonic leucine zipper kinase (MELK) is a member of the sucrose-non-fermenting/AMP-activated protein kinase family of serine-threonine protein kinases and plays key functional roles in multiple cellular processes, including the cell cycle, cell proliferation, apoptosis, and cell migration (8-11). MELK is overexpressed in a variety of human tumors, including melanoma (12), breast (13), gastric (11), and high-grade prostate cancer (14), as well as glioblastoma multiforme (15). High levels of MELK expression are associated with poor prognoses in patients (14,16). Inhibition of MELK has been demonstrated to suppress tumor growth *in vitro* and in pre-clinical adult cancer models (17-19). MELK is also elevated in cancer stem cells (CSCs) and can promote CSC growth (20). Small molecule inhibitors of MELK have anticancer activity in breast and other cancers (20-22), indicating that MELK may be a target for cancer therapy. A recent study reported that MELK enhances tumorigenesis and metastasis of ESCC cells via activation of the FOXM1 signaling pathway (23).

Epithelial-mesenchymal transition (EMT) is a biological process that is known to be crucial for embryogenesis, wound healing and malignant progression (24). In the context of cancer pathogenesis, EMT confers on cancer cells increased tumor-initiating and metastatic potential (25). EMT can be

induced by several intracellular signaling pathways, including the transforming growth factor-β (TGFβ), WNT, PI3K/AKT and nuclear factor-κB (NF-κB) pathways (24). NF-κB is a ubiquitous transcription factor that plays a prominent role in mediating EMT (26). NF-κB can be activated in neoplastic cells by a series of cell intrinsic and extrinsic signals (e.g., genetic alterations and microenvironmental cytokines, respectively). Subsequently, nuclear NF-κB promotes EMT by inducing the expression of EMT-inducing transcription factors (EMT-TFs), including Snail, zinc finger E-box-binding homeobox (ZEB)1, ZEB2 and TWIST1, and by directly inducing the expression of mesenchymal proteins such as CD44, vimentin and N-cadherin (27).

The prognostic role of MELK in ESCC and the precise molecular mechanisms by which it promotes EMT and aggressive progression in ESCC remain unknown. Whether there are other MELK downstream signaling pathways besides FOXM1 in ESCC and whether MELK promotes ESCC metastasis by activating NF-κB were investigated in the present study.

Materials and methods

Patients and tissue samples. A total of 84 samples of ESCC tissue (including 84 cases of tumor tissues and 18 adjacent normal esophageal tissues) were obtained from Meizhou People's Hospital (Meizhou, China) between September 2004 and February 2008. None of the patients were treated by radiotherapy or chemotherapy before surgical operation. All samples were collected with written informed consent and approved by the Research Ethics Committee of Meizhou People's Hospital. The histopathological diagnosis was performed according to the World Health Organization criteria. Tumor staging was determined based on the 6th edition of the tumor-node-metastasis (TNM) classification of the International Union Against Cancer (IUAC) (28). The characteristics of the patients are detailed in Table I.

Immunohistochemistry (IHC). Tissues were fixed in 10% neutral buffered formalin overnight at room temperature (RT) and embedded in paraffin. The 5-μm-thick sections of tissue paraffin samples were prepared on pathological sections for immunohistochemical staining. Tissue sections were heated in citrate buffer solution (pH 6.0) at 100˚C for 10 min to facilitate antigen retrieval. After tissue samples cooled down to RT, the endogenous peroxidase activity was blocked by incubating sections with 10% normal goat serum (product no. C0265; Beyotime Institute of Biotechnology) for 1 h at RT followed by incubation with an antibody against MELK (1:300; cat. no. 11403-1-AP; ProteinTech Group, Inc.) for 3 h at RT, and incubated with a secondary antibody (Dako REAL EnVision; cat. no. K5007; Agilent Technologies, Inc.) for 30 min at RT after rinsing with PBS. Immunoreacted cells were visualized using diaminobenzidine, and nuclei were counterstained with hematoxylin for 10 min at RT. The results were independently assessed by two pathologists, neither of whom knew the clinical data. The percentage of positive cells in the sections was evaluated as 0-100%, while cases with >20% of tumor cells exhibiting strong cytoplasmic staining were considered positive MELK staining. A negative control tissue section without primary MELK antibody was also included (Fig. S1). Leica Microsystems DM6000B light microscope (Leica Microsystems GmbH) was used for evaluation and image recording.

Cell lines and cell culture. Human normal esophageal epithelial cell line Het-1A (cat. no. CC-Y1220) was purchased from Shanghai EK-Bioscience Biotechnology Co., Ltd. (http://www.elisakits.cn/index.php). Human ESCC cell lines KYSE140 (BNCC no. BNCC351870), KYSE450 (BNCC no. BNCC339896) and KYSE510 (BNCC no. BNCC360126) were purchased from BeNa Culture Collection; Beijing Beina Chunglian Institute of Biotechnology (https://www.bncc.org.cn/). KYSE150 (TCHu236) was obtained from the Shanghai Institute of Cell Biology, Chinese Academy of Sciences. Cells were cultured in RPMI-1640 medium (Biological Industries) with 10% fetal bovine serum (Biological Industries) and 1% penicillin-streptomycin (Beyotime Institute of Biotechnology) in a humidified atmosphere containing 5% CO_2 at 37˚C. For pharmacological inhibition of MELK, ESCC cells were treated with 4-16 nM of MELK inhibitor OTSSP167 (cat. no. S7159; Selleck Chemicals) for 24-32 h at 37˚C.

RNA extraction and reverse transcription-quantitative PCR (RT-qPCR). Total cellular RNA was obtained using TRIzol (Invitrogen, Thermo Fisher Scientific, Inc.) according to the manufacturer's instructions, and complementary DNA (cDNA) was prepared from 1 μg of total RNA using PrimeScript RT reagent Kit with gDNA Eraser (cat. no. RR047A; Takara Bio, Inc.) according to the manufacturer's instructions. RT-qPCR was performed for the gene fold change using SYBR Premix Ex Taq™ (cat. no. RR820A; Takara Bio, Inc.). Thermocycling conditions were as follows: Initial denaturation of 30 sec at 95˚C; followed by 40 cycles of denaturation at 95˚C for 5 sec, and annealing and extension at 60˚C for 30 sec. The mRNA levels were analyzed by the comparative $2^{-\Delta\Delta Cq}$ method after normalization to GAPDH (29). The primer sequences used in this research were as follows: MELK forward, 5'-TGATGA TTGCGTAACAGAAC-3' and reverse, 5'-GAAGATAGGTAG CCGTGAG-3'; human GAPDH forward, 5'-ATCAATGGA AATCCCATCACCA-3' and reverse, 5'-GACTCCACGACG TACTCAGCG-3'.

Plasmid constructs and transfection. Corresponding short hairpin RNA (shRNA) oligonucleotide sequences were cloned into the PLKO.1-TRC vector (Sigma-Aldrich; Merck KGaA) to obtain an empty vector as the control and the generation of lentiviral vectors encoding shRNA targeting MELK. The targeting sequences of shMELK and shNC were as follows: shMELK-1, 5'-GCCTGAAAGAAACTCCAATTA-3'; shMELK-2, 5'-CTG AGTTAATACAAGGCAAAT-3'; shMELK-3, 5'-CAGAAA CAACAGGCAAACAAT-3'; sh negative control (NC), 5'-TTC TCCGAACGTGTCACGT-3'. A total of 12 μg lentiviral expression vectors and second-generation lentiviral packaging vectors pSPAX2 and pMD2.G (Addgene, Inc.) were transfected into 293T (cat. no. SCSP-502; Shanghai Cell Bank of the Chinese Academy of Sciences) cells at a ratio of 4:3:2 and cultured at 37˚C. The virus was collected three times at an interval of 24 h between collections. ESCC cells were infected with lentiviral particles (MOI=20) for 24 h in the presence

Table I. Association between MELK expression and clinicopathological features in 84 patients with ESCC.

Variables	No. of cases	MELK expression		P-value
		Negative	Positive	
Sex				0.034[a]
Male	67	28	39	
Female	17	12	5	
Age (years)				0.662
≤55	42	19	23	
>55	42	21	21	
Tumor size (cm)				0.393
≤5.0	44	19	25	
>5.0	40	21	19	
Histological grade				0.656
I	12	5	7	
II-III	72	35	37	
T stage				0.447
T1-T2	24	13	11	
T3-T4	60	27	33	
N stage				0.596
N0	50	25	25	
N1	34	15	19	
Tumor stage				0.297
I-II	54	28	26	
III-IV	30	12	18	

[a]Statistically significant. MELK, maternal embryonic leucine zipper kinase; ESCC, esophageal squamous cell carcinoma.

of polybrene (5 μg/ml; cat. no. TR-1003; Sigma-Aldrich; Merck KGaA). Following selection by 2.5 mM puromycin (Sigma-Aldrich; Merck KGaA) for 3 days, the cells with stable knockdown of MELK were selected and maintained in 1 mM puromycin. Western blotting was then performed to identify the knockdown of MELK. For overexpression of inhibitor of nuclear factor-κB kinase subunit β (IKKβ; MELK-depleted ESCC cells were transfected with 2 μg IKKβ expression plasmid (pcDNA3.1-IKKβ) or the empty vector (pcDNA 3.1-EV) as the control. Following selection using 400 μg/ml G418 (MedChemExpress) for 2 weeks, the cells with stable overexpression of IKKβ were selected and maintained in 200 μg/ml G418.

Proliferation assays with Cell Counting Kit-8 (CCK-8). CCK-8 assays were performed according to the manufacturer's instructions, to detect cell proliferation. KYSE150 and KYSE510 cells were seeded into 96-well plates with a density of 1,000 cells/well in 100 μl cell medium. Each group was assessed every 24 h. The plates were placed in a 37˚C incubator for 2 h after adding 10 μl of CCK-8 working solution (Bimake), and then the absorbance was measured at 450 nm using a microplate reader. The average values of the five replicates were calculated and used to draw the growth curve. This experiment was repeatedly performed three times. The OD_{450} value was statistically evaluated by one-way ANOVA analysis followed by Tukey's post hoc test using SPSS 19.0 statistical software.

Colony formation assay. Colony formation assays were performed to detect cell proliferation. KYSE150 and KYSE510 cells were inoculated into 6-well plates with a concentration of 100 cells/well. The plates were placed in a cell incubator at 37˚C for 2 weeks, and the medium with 10% FBS was renewed every 4 days. When visible colonies had formed, each well was fixed with 1 ml of 4% paraformaldehyde for 30 min at RT and stained with 1 ml of 0.1% crystal violet (Beyotime Insitute of Biotechnology) for 30 min at RT. The number of visible colonies (consisting of >50 cells) of three replicates was counted manually after the plates dried up. The experiment was independently performed three times.

Transwell assays. Transwell assays were performed to detect cell vertical migration and invasion. A total of $5x10^4$ KYSE150 and KYSE510 cells in 150 μl serum-free medium were seeded in the upper compartment of an 8-μm pore size Transwell chamber (Corning, Inc.) after pre-treatment with serum-free medium for 12 h. The upper chambers had been pre-coated with 50 μl of 2.5 mg/ml solution of Matrigel at 37˚C for 1 h (Corning, Inc.) for the invasion assays or uncoated for the migration assays. The lower chambers were filled with 600 μl RPMI-1640 medium containing 10% FBS. After 24 h (migration experiment) or 36 h (invasion experiment), the cells on the upper surface of the chamber membranes were wiped off. The membranes were then fixed with 4% polymethanol at RT for 30 min and stained with 0.5% crystal violet at RT for 30 min. Five fields randomly selected under a light microscope were captured to count the cells on the lower surface of the filter at a magnification of x100. This experiment was performed in triplicate independently.

Wound healing assays. Wound healing assays were performed to detect cell lateral migration. A total of $5x10^5$ KYSE150 and KYSE510 cells were seeded in a 6-well plate and exposed to serum-free RPMI-1640 medium for 12 h to inhibit cell proliferation. When the confluency reached >80%, a horizontal scratch was made using a sterile 200-μl microliter pipette tip. After the wound was induced, the cells were washed twice with PBS and cultured in a serum-free medium. Images of migration were obtained at 0, 16, and 20 h after inducing under a light microscope. The assays were repeatedly performed three times.

Western blotting. Western blotting was performed to detect the expression level of related proteins. The whole KYSE150 and KYSE510 cell lysates were prepared in SDS buffer with 1% protease inhibitor cocktail and 1% PMSF. The nuclear proteins were obtained using Nuclear and Cytoplasmic Protein Extraction Kit (Beyotime Institute of Biotechnology) according to the manufacturer's instructions. The concentration of protein samples was quantified using BCA Protein Assay Kit (Beyotime Institute of Biotechnology). A total of 50 μg of proteins were separated by 10% SDS-PAGE and then transferred onto PVDF membranes. Incubated with TBST

buffer (Tris-buffered saline with 0.1% Tween-20) including 5% dried skimmed milk at RT for 1 h, the corresponding PVDF membranes were incubated with a primary antibody at 4˚C overnight. The membranes were then incubated with horseradish peroxidase-conjugated secondary antibodies (1:2,000; product no. 7074; Cell Signaling Technology, Inc.) at RT for 1 h. Finally, protein bands were detected using enhanced chemiluminescence (ECL) detection reagent (MilliporeSigma) according to the manufacturer's instructions. The gray-scale value of the immunoreactive bands was measured by ImageJ (version 1.53; National Institutes of Health). Antibodies used in this study were as follows: Antibodies against zonula occludens-1 (ZO-1; 1:1,000; product no. 8193), E-cadherin (1:1,000; product no. 14472), N-cadherin (1:1,000; product no. 13116), matrix metalloproteinase (MMP)-2 (1:1,000; product no. 40994), MMP-9 (1:1,000; product no. 13667), ZEB2 (1:1,000; product no. 97885), Slug (1:1,000; product no. 9585), Snail (1:1,000; product no. 3879), phosphorylated (p)-IKKα/β (Ser176/180; 1:1,000; product no. 2697) were purchased from Cell Signaling Technology, Inc. Antibodies against GAPDH (1:1,000; cat. no. 60004-1-Ig), MELK (1:2,000; cat. no. 11403-1-AP), p65 (1:1,000; cat. no. 10745-1-AP) were obtained from ProteinTech Group, Inc. Antibodies against NF-κB1 (1:500; cat. no. BM3946) and NF-κB2 (1:500; cat. no. BA1298) were purchased from Boster Biological Technology. Antibodies against p-p65 (Ser536; 1:1,000; cat. no. WL02169) and p-IKB-α (Ser32/36; 1:500; cat. no. WL02495) were purchased from Wanleibio Co., Ltd. Antibody against p62 (SQSTM1) (1:1,000; cat. no. PM045) were obtained from MBL Beijing Biotech Co., Ltd.

Immunofluorescence staining. A total of $4x10^4$ KYSE150 and KYSE510 cells were singly seeded on coverslips in 24-well plates and fixed with 4% paraformaldehyde at RT for 20 min. After being washed thrice with PBS for 5 min each time, cells were permeabilized with 0.3% Triton X-100 (Sigma-Aldrich; Merck KGaA) in PBS for 10 min at 4˚C and blocked with 10% goat serum in PBS at RT for 60 min. Cells were incubated with a primary antibody overnight at 4˚C and then were incubated with Alexa Fluor 488/647-conjugated secondary antibodies (1:500; product nos. 4412 and 4414; Cell Signaling Technology, Inc.) at RT for 1 h. Following washing three times with PBS for 10 min each time, cells were counterstained with DAPI for 15 min at RT. Fluorescence images were captured by Zeiss LSM 780 or LSM 800 laser scanning microscope (Carl Zeiss AG). Antibodies used in this study were as follows: MELK (1:100; cat. no. 11403-1-AP; ProteinTech Group, Inc.), Slug (1:100; product no. 9585; Cell Signaling Technology, Inc.), NF-κB1 (1:25; cat. no. BM3946; Boster Biological Technology), and NF-κB2 (1:50; cat. no. BA1298; Boster Biological Technology).

Co-immunoprecipitation (Co-IP) assays. Protein lysate of KYSE510 cells was collected using IP lysis buffer (cat. no. P0013; Beyotime Insitute of Biotechnology) and mixed with the indicated antibody or negative control IgG overnight at 4˚C. Subsequently, 200 μl lysate was mixed with 20 μl of protein G magnetic beads (cat. no. 37478; Cell Signaling Technology, Inc.) for 4 h at 4˚C; the binding complex was obtained using a magnetic stand. After being washed thrice with IP buffer, the complex was boiled for 5 min at 100˚C with SDS buffer and centrifuged at 4˚C and 12,000 x g for 2 min to gain bound protein samples, which were used for western blotting. Antibodies used in this study were as follows: MELK (1:50; cat. no. 11403-1-AP; ProteinTech Group, Inc.), IKKα/β (1:50; cat. no. WL01900; Wanleibio Co., Ltd.), and IgG (1:50; cat. no. A7016; Beyotime Institute of Biotechnology).

Bioinformatics analysis. Two human microarray datasets, namely, GSE20347 (30) and GSE23400 (31), were obtained from the public Gene Expression Omnibus (GEO) database (http://www.ncbi.nlm.nih.gov/geo). The mRNA sequencing data of patients with ESCC were downloaded from The Cancer Genome Atlas (TCGA) database (https://portal.gdc.cancer.gov/). Gene expression of MELK in the GEO database and TCGA ESCC database were assessed using GraphPad Prism 7 software (GraphPad Software, Inc.). Gene set enrichment analysis (GSEA) was performed by generating the Gene MatriX file (.gmx) using published signatures for the Rickman *et al* 'metastasis' (32), the Sarrio *et al* 'epithelial mesenchymal transition' (33), and GO biological process gene sets from the Molecular Signatures Database (MSigDB; version 6.2) (34). The gene cluster text file (.gct) was generated from the TCGA ESCC database. The number of permutations for GSEA was set to 1,000, and the TCGA gene list was used as the chip platform.

Experimental in vivo metastasis assays. A total of 14 male BALB/c-nu/nu mice (aged 4 to 5 weeks; weighing 18 to 25 g) were purchased from the Shanghai Laboratory Animal Center of the Chinese Academy of Sciences and raised in a pathogen-free laminar flow cabinet throughout the experiments under the following conditions: Controlled humidity, 50±10%; temperature, 23±2˚C; 12-h light/dark cycle and *ad libitum* access to food and water. KYSE150 cells stably transfected with shNC or shMELK were collected and re-suspended in PBS at a concentration of $1x10^8$ cells/ml. Prepared cells were injected into the tail veins of 14 mice (100 μl per mouse). The health and behavior of the nude mice was monitored every 2 days. The mice would be humanely euthanized if they experienced unrelieved pain or distress, based on the euthanasia criteria. Following 5 weeks of injection, the mice were euthanized by cervical dislocation. The lungs and livers of the mice were removed and photographed. The visible tumors on the surface of the lung tissue were then counted. The largest diameter of the tumor nodules was 2 mm, and fusion nodules exceeding 2 mm were calculated as the diameter/2 mm. The experiment was strictly carried out following the Guide for the Care and the Use of Laboratory Animals of the National Institutes of Health and was approved by the Animal Care and Experimental Ethics Committee of Jinan University (approva l no. IACUC-20190211-04; Guangzhou, China).

Statistical analysis. All data were analyzed with SPSS 19.0 software (IBM Corp.). The association between MELK expression and clinicopathological feathers of patients with ESCC was analyzed using the chi-squared test. The Kaplan-Meier method and log-rank tests were used to compare the overall survival. The numerical data are reported as the mean ± standard deviation (SD). The difference between two groups was

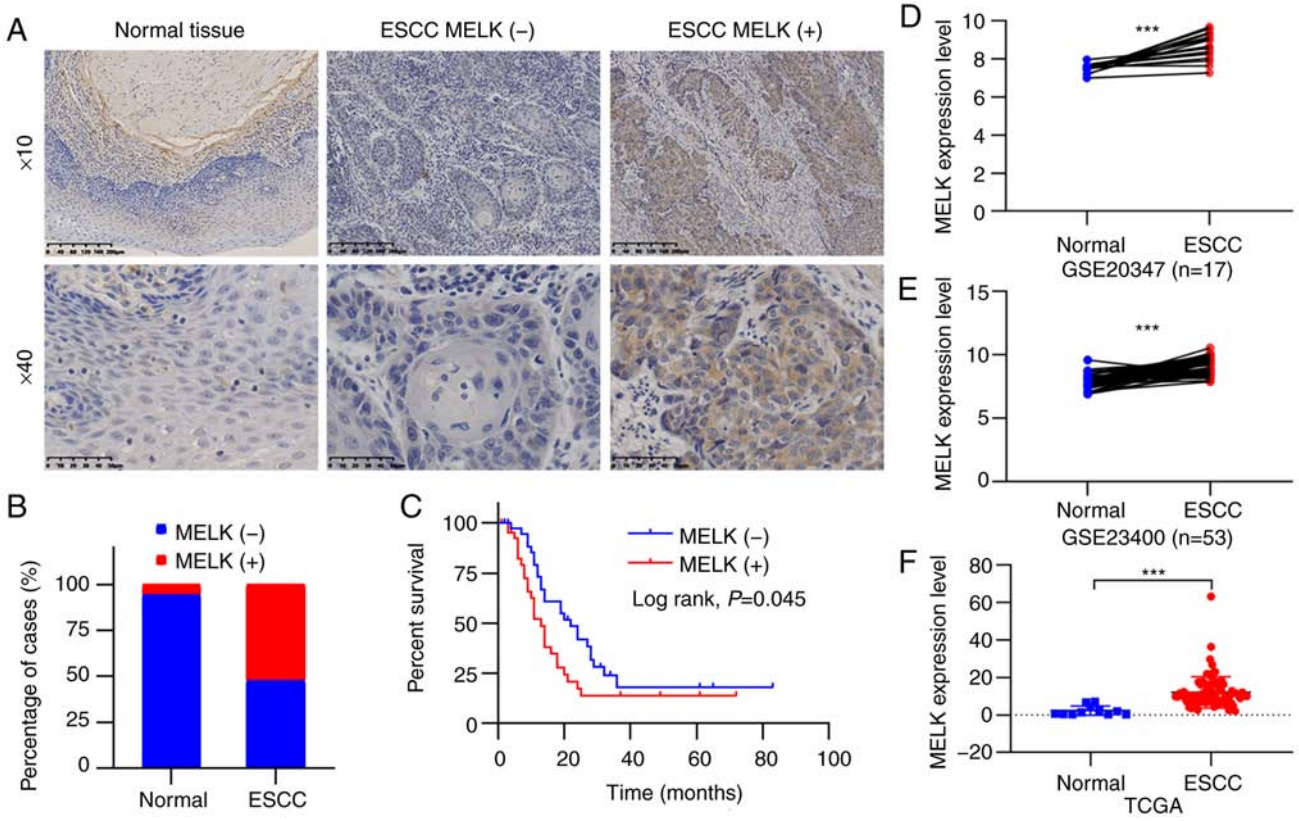

Figure 1. MELK expression is elevated and associated with poor prognosis in ESCC. (A) Representative MELK immunohistochemical staining of ESCC and normal esophageal tissue (magnification, x10 and x40). Scale bars, 50 μm or 200 μm. (B) The histogram shows the percentage of MELK immunostaining in ESCC and normal esophageal tissue. ESCC tissues exhibited significantly higher MELK expression levels than normal esophageal tissue (Chi-square test, P<0.001). (C) Kaplan-Meier curves according to MELK expression status in ESCC. Patients with positive MELK expression had a shorter overall survival time than patients with negative MELK expression (log-rank test, P=0.045). (D-E) The relative expression of MELK in ESCC tissues and paired normal tissues were compared using GEO datasets, series GSE20347 and GSE23400. (F) The relative expression of MELK in ESCC tissues and normal tissues was compared using TCGA data. ***P<0.001. MELK, maternal embryonic leucine zipper kinase; ESCC, esophageal squamous cell carcinoma; GEO, Gene Expression Omnibus; TCGA, The Cancer Genome Atlas.

analyzed by a two-tailed unpaired Student's t-test. A one-way ANOVA with Tukey's post hoc test were used to analyze three or more groups. P-values <0.05 were considered to indicate a statistically significant difference.

Results

MELK is highly expressed in human ESCC tissues and is associated with poor overall survival of patients with ESCC. MELK is highly expressed in cancer and plays key roles in tumor progression in some cancer types (11,12); however, the role of MELK in ESCC remains unknown. To assess the roles of MELK in ESCC, the expression levels of MELK in 84 ESCC tissues and 18 adjacent normal esophageal tissues were first assessed by immunohistochemical staining. The MELK protein was found to be localized in the cytoplasm (Fig. 1A). The positive rates of MELK protein detection were 5.6% (1/18) in non-tumor tissues and 52.4% (44/84) in tumor tissues, and the expression of MELK was significantly upregulated in ESCC compared with normal tissues (P<0.001; Fig. 1B). The associations between the expression status of MELK and clinicopathological characteristics of patients were also analyzed, although the results revealed that positive MELK expression was not significantly associated with characteristics, including age, histological grade, and tumor stage (P>0.05; Table I). By using Kaplan-Meier analysis, it was determined that positive MELK expression indicated the poor overall survival of patients with ESCC (P<0.05; Fig. 1C). Furthermore, the GEO and TCGA databases were searched to analyze MELK levels in patients with ESCC, and the increased expression of MELK was also observed in ESCC (Fig. 1D-F). These results indicated that the expression of MELK protein was elevated in ESCC and predicted a poor prognosis in patients.

MELK inhibition reduces proliferation and colony formation in ESCC cells. The aforementioned results revealed that MELK was more highly expressed in ESCC and positively associated with the poor survival of patients. To determine the biological function of MELK in ESCC, the protein level of MELK in ESCC cell lines was first analyzed, and then KYSE150 and KYSE510 cell lines, which had higher expression levels of MELK and represented poorly differentiated and well differentiated ESCC respectively, were selected (35), to be used for further study (Fig. 2A). Stable knockdown of MELK was generated by transfecting KYSE150 and KYSE510 cells with shRNA of MELK. Following transfection and selection with puromycin, the expression of MELK in KYSE150 and KYSE510 cells was significantly decreased (Fig. 2B). The effect of MELK on the proliferation of ESCC cells was then investigated using CCK-8 assays. The results revealed that

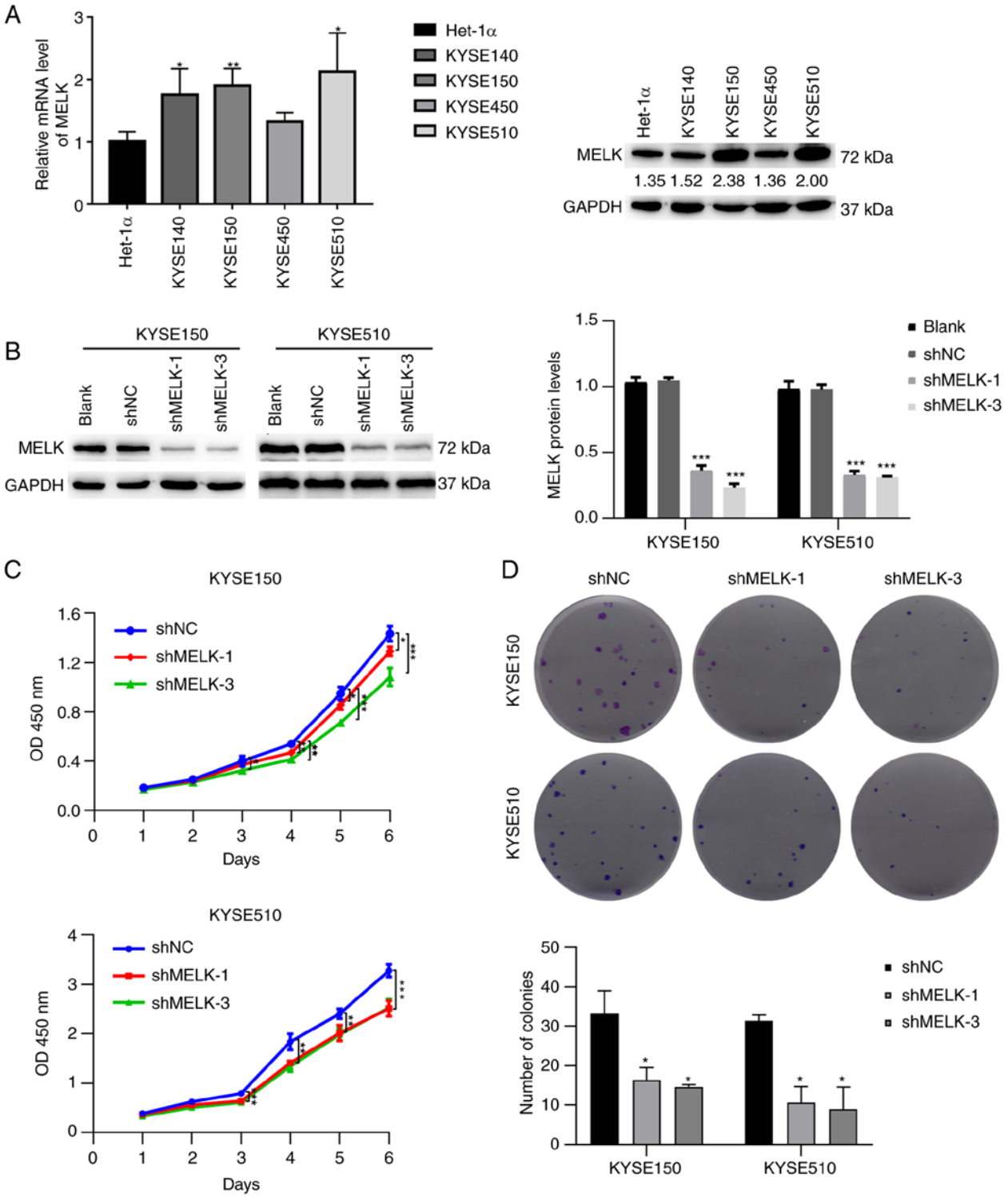

Figure 2. Knockdown of MELK inhibits cell proliferation of ESCC cells. (A) The expression levels of MELK in ESCC cell lines. (B) The knockdown efficiency of MELK short hairpin RNA was confirmed by western blotting in KYSE150 and KYSE510 cells. (C) Cell Counting Kit-8 assays were performed to detect cell proliferation. (D) Colony formation assays were performed to detect cell proliferation. The histograms reveal the number of colonies counted. Data are presented as the mean ± SD of 3 independent experiments. *P<0.05, **P<0.01 and ***P<0.001. MELK, maternal embryonic leucine zipper kinase; ESCC, esophageal squamous cell carcinoma; sh, short hairpin RNA; NC, negative control.

knockdown of MELK significantly reduced the growth of KYSE150 and KYSE510 cells compared with the control cells (Fig. 2C). Colony formation assays demonstrated that knockdown of MELK efficiently decreased the ability of ESCC cells to proliferate (Fig. 2D). These results indicated that MELK regulated the proliferative ability of ESCC cells.

MELK inhibition decreases the migration and invasion of ESCC cells. Next, the cell migration and invasive abilities of cells were examined using Transwell migration and invasion assays, as well as wound healing assays. The number of migrated and invasive cells in MELK-knockdown KYSE150 and KYSE510 cells was significantly decreased compared

with the control cells (Fig. 3A and B). In the wound healing assays, the control cells markedly closed the wound 16 h after scratching, but MELK-knockdown cells were unable to heal the wound, and the wound areas of the experimental groups and controls were significantly different. MELK knockdown significantly inhibited cell migration (Fig. 3C). To further ascertain whether MELK accelerates the motility capacity of ESCC cells, GSEA was used to determine the degree of MELK expression with metastasis-related signatures. The results showed that ESCC with high MELK expression had significant enrichment with an aggressive signature. To further confirm this observation, MELK expression was examined with metastasis-related markers and it was determined that GSEA highlighted the positive association of increased MELK expression with metastasis and the negative association of increased MELK expression with adherens junction and tight junction (Fig. 3D). Collectively, these findings indicated that high MELK expression may be associated with the highly infiltrative and aggressive characteristics of ESCC cells.

MELK facilitates the EMT in ESCC cells. EMT is an early event in tumor metastasis, and tumor cells show enhanced migration and invasion abilities during the EMT (24,25). Therefore, the expression of markers associated with EMT were examined using western blotting. MELK inhibition upregulated the expression of epithelial-related proteins, including E-cadherin and ZO-1, and downregulated mesenchymal-related protein N-cadherin in both KYSE150 and KYSE510 cells (Fig. 4A). Moreover, EMT-TFs, ZEB2, Slug and Snail, were also inhibited after MELK knockdown (Fig. 4B). In particular, the protein expression of Slug was demonstrated to be markedly reduced by immunofluorescence staining (Fig. 4C). In addition, MELK knockdown decreased MMP-9 and MMP-2 protein levels, which are involved in facilitating cell metastasis by extracellular matrix (ECM) degradation (Fig. 4A). Furthermore, GSEA highlighted the positive association of increased MELK expression with the EMT signature (Fig. 4D). Thus, the results demonstrated that MELK may promote cell migration and invasion by promoting EMT in ESCC cells.

MELK positively regulates NF-κB signaling. To decipher the mechanisms by which MELK regulates EMT, GSEA was used to compare the expression profiles between high- and low-MELK expression cases. The NF-κB-activated gene signature was enriched in high-MELK expression cases (Fig. S2A). Aberrant NF-κB pathway activation is a significant contributor to the EMT (36,37). The NF-κB pathway can directly and indirectly affect Snail, Slug, and ZEB1 expression to facilitate the EMT. The expression/phosphorylation of proteins involved in the NF-κB signaling were examined by western blotting. The knockdown effect of MELK on various pathways involved in EMT, including WNT/β-catenin, TGFβ and AKT signaling pathways, were also assessed to search for the downstream pathway of MELK. The results demonstrated that MELK inhibition significantly downregulated the expression of main NF-κB subunits, including NF-κB p50, NF-κB p52, NF-κB p65, and phosphorylated NF-κB (p-NF-κB) p65 (Fig. 5A), but it did not affect the expression of β-catenin, p-SMAD2 and p-AKT (Fig. S2B). The nuclear translocation of NF-κB p65, NF-κB p50, and NF-κB p52 was also examined, and MELK inhibition led to decreased translocation of NF-κB p65, NF-κB p50, and NF-κB p52 to the nucleus (Fig. 5B-C), which suggested downregulation of this signaling pathway. Additionally, Slug, the downstream target of the NF-κB pathway was evaluated, and its expression was shown to be reduced in the nucleus (Fig. 5B). These results suggested that MELK knockdown inhibited activation of the NF-κB pathway. NF-κB complex is usually inactive and located in the cytoplasm while bound to IκB inhibitor proteins (27). When IκB protein is phosphorylated by the IκB kinase (IKK) complex, which leads to IκB ubiquitination and subsequent degradation, NF-κB subunits may translocate to the nucleus and activate downstream gene transcription (27). Thus, the expression levels of NF-κB upstream kinases were examined; the results revealed that MELK inhibition reduced the protein levels of p-IκB, p-IKK, and p62 by which the activation of NF-κB was decreased (Fig. 5D). Furthermore, co-immunoprecipitation in ESCC cells was performed to detect the interaction between MELK and the upstream kinases of the NF-κB signaling and it was determined that MELK could bind to IKK and regulated phosphorylation of IKK (Fig. 5E). Hence, the results suggested that MELK may activate the canonical NF-κB signaling by interacting with IKK.

Overexpression of IKKβ rescues NF-κB signaling and the migration of ESCC cells after MELK inhibition. Because IKKβ acts downstream of MELK, it was investigated whether ectopic expression of IKKβ could rescue the inhibition of NF-κB signaling caused by MELK inhibition. IKKβ-overexpressing plasmid was stably transduced into MELK-depleted ESCC cells, and then the expression of IKKβ was detected by western blotting. As revealed in Fig. 6A, the protein levels of p-IKKβ, IKKβ and its downstream targets including p-IκBα, p-p65 and NF-κB p50 were markedly upregulated by IKKβ in ESCC cells with MELK depletion. A previous study reported that MELK promoted tumor growth and metastasis via stimulating FOXM1 signaling in ESCC (23). In view of the reciprocal regulation between NK-κB and FOXM1 (38), the expression of FOXM1 in ESCC cells with MELK knockdown and IKKβ overexpression was also assessed. As revealed in Fig. 6A, MELK knockdown inhibited FOXM1 expression, which was rescued by IKKβ overexpression. Immunoblotting analysis also revealed that ectopic expression of IKKβ markedly restored Slug, E-cadherin, N-cadherin, ZO-1, MMP-2 and MMP-9 expression in MELK-depleted ESCC cells (Fig. 6B). Moreover, overexpression of IKKβ in MELK-depleted ESCC cells also attenuated the inhibitory effects on the migration in both Transwell and wound healing assays (Fig. 6C and D). By contrast, the expression of an empty vector did not rescue the migration of ESCC cells (Fig. 6C and D). Collectively, these results demonstrated that attenuation of NF-κB signaling was partly responsible for blocking ESCC migration inhibition after MELK inhibition.

MELK inhibitor blocks the EMT via NF-κB pathway. To further confirm whether MELK inhibition, but not an off-target effect, would reduce the activation of the NF-κB pathway, ESCC cell lines were treated with the MELK inhibitor OTSSP167 (16,39,40). OTSSP167 treatment significantly inhibited ESCC cell migration ($P<0.05$; Fig. 7A). OTSSP167

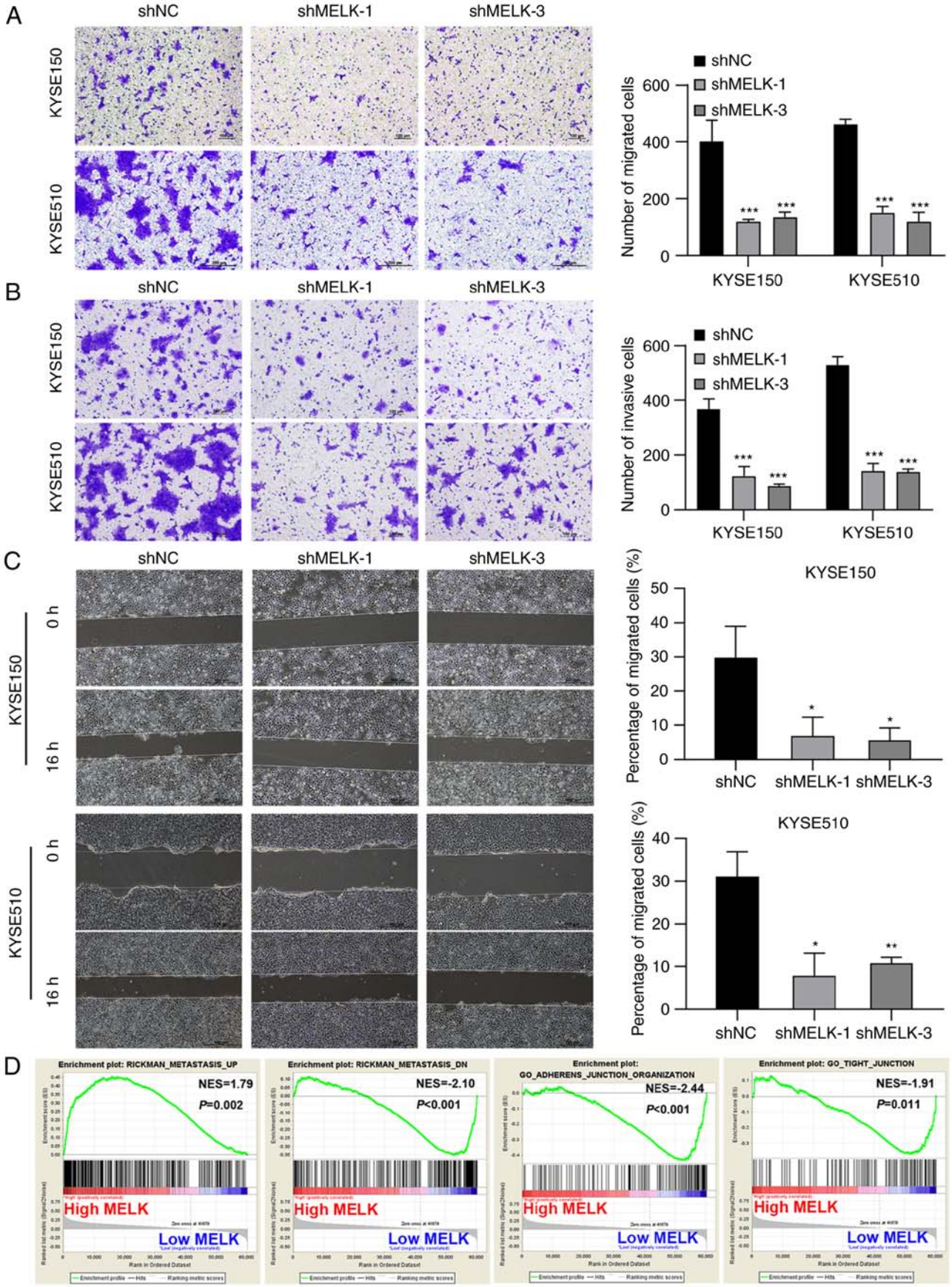

Figure 3. Knockdown of MELK inhibits cell invasion and migration abilities of ESCC cells. (A and B) Representative Transwell migration (A) and invasion (B) images and statistical analysis of the number of counted KYSE150 and KYSE510 cells with MELK knockdown. Scale bars, 100 μm or 200 μm. (C) Micrographs and histograms of the scratch wound-healing assay of ESCC cells with MELK knockdown. Scale bars, 500 μm. (D) GSEA was performed using the signatures for the Rickman *et al* 'metastasis' and GO biological process gene sets. Patients were separated by high or low MELK mRNA expression. Data are presented as the mean ± SD of 3 independent experiments. *P<0.05, **P<0.01 and ***P<0.001. MELK, maternal embryonic leucine zipper kinase; ESCC, esophageal squamous cell carcinoma; GSEA, gene set enrichment analysis; sh, short hairpin RNA; NC, negative control; NES, normalized enrichment score.

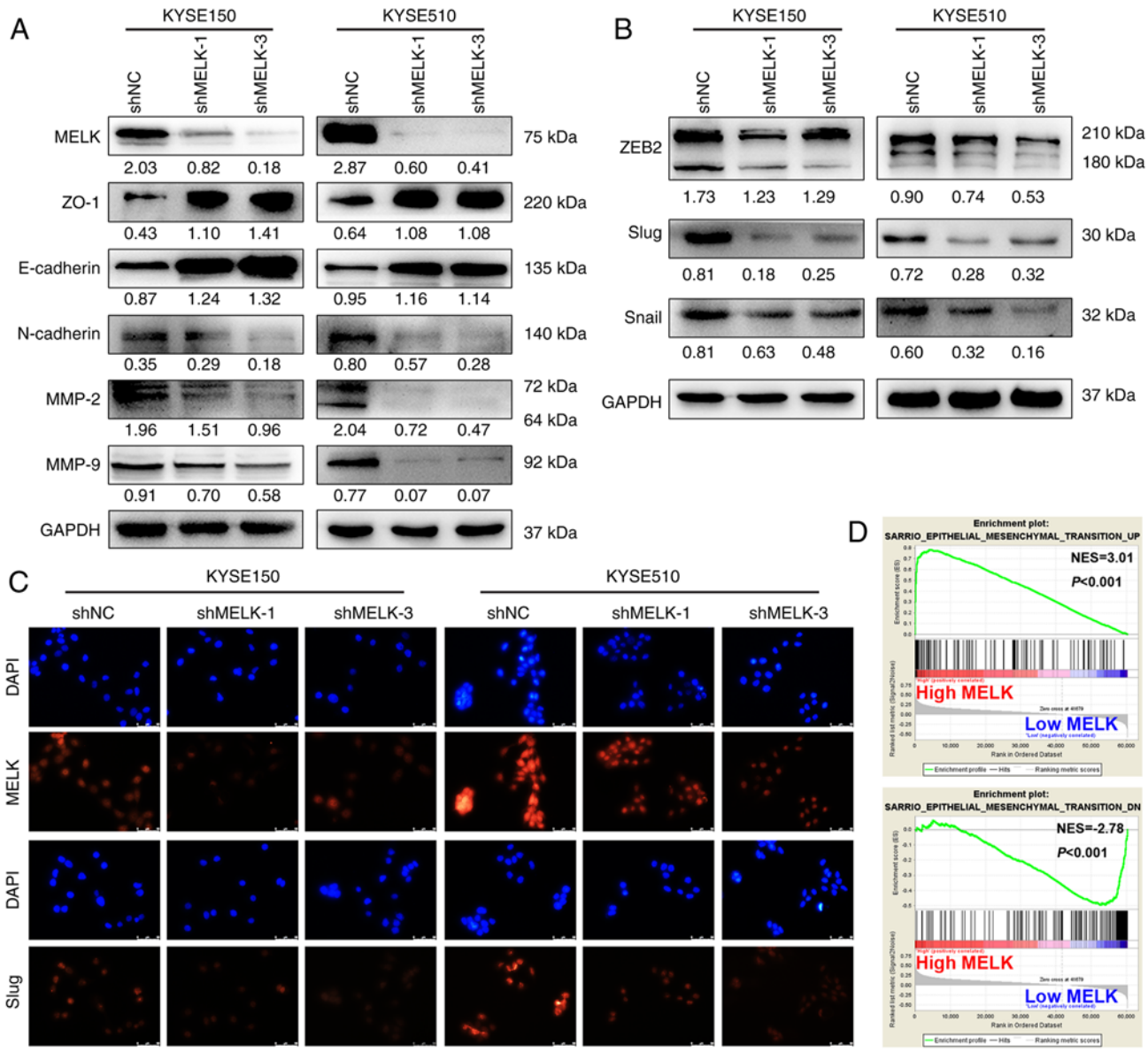

Figure 4. MELK promotes the migration and invasion abilities of ESCC cells by regulating the expression of EMT-associated proteins. (A and B) Western blot analysis of EMT-associated proteins in ESCC cells with MELK knockdown. (C) Immunofluorescence staining of MELK and Slug protein in ESCC cells. Scale bars, 50 μm. (D) GSEA was performed using the signatures for the Sarrio *et al* 'epithelial mesenchymal transition'. Data are presented as the mean ± SD of 3 independent experiments. MELK, maternal embryonic leucine zipper kinase; ESCC, esophageal squamous cell carcinoma; EMT, epithelial-mesenchymal transition; GSEA, gene set enrichment analysis; sh, short hairpin RNA; NC, negative control.

reduced the protein levels of p-IKK, p-IκB, NF-κB1 p50, NF-κB2 p52, p62, and p-NF-κB p65 and the downstream protein Slug (Fig. 7B-C). Thus, MELK inhibition was confirmed to block the EMT by decreasing the activation of NF-κB signaling in ESCC cells.

Knockdown of MELK inhibits metastatic capacities of ESCC cells in vivo. To determine whether MELK regulates ESCC cell migration and invasion potential *in vivo*, KYSE150-shMELK and control KYSE150 vector cells were injected into the tail vein of nude mice (seven mice per group). At 5 weeks after cell injection, mice were sacrificed, and metastatic tumors formed in the lung and liver were examined. The results showed that no tumor nodule was formed in the liver of mice. However, metastatic tumor nodules were frequently observed in the lung of mice, and knockdown of MELK significantly decreased the number of metastatic nodules in the lung (P<0.05; Fig. 8A-C). These results demonstrated that MELK inhibition significantly reduced metastasis of ESCC.

Discussion

Recent studies have shown that MELK plays an important role in tumor progression of numerous types of tumors (11,14,16,41). However, little is known about the function and related mechanisms of MELK in ESCC (23). In the present study, it was demonstrated that MELK expression was upregulated in ESCC tissues and was important for the acquisition of an aggressive and poor prognostic phenotype. It was also demonstrated that MELK inhibition decreased cell proliferation, migration, and invasion of ESCC cells both *in vitro* and *in vivo*. Furthermore, it was observed that MELK

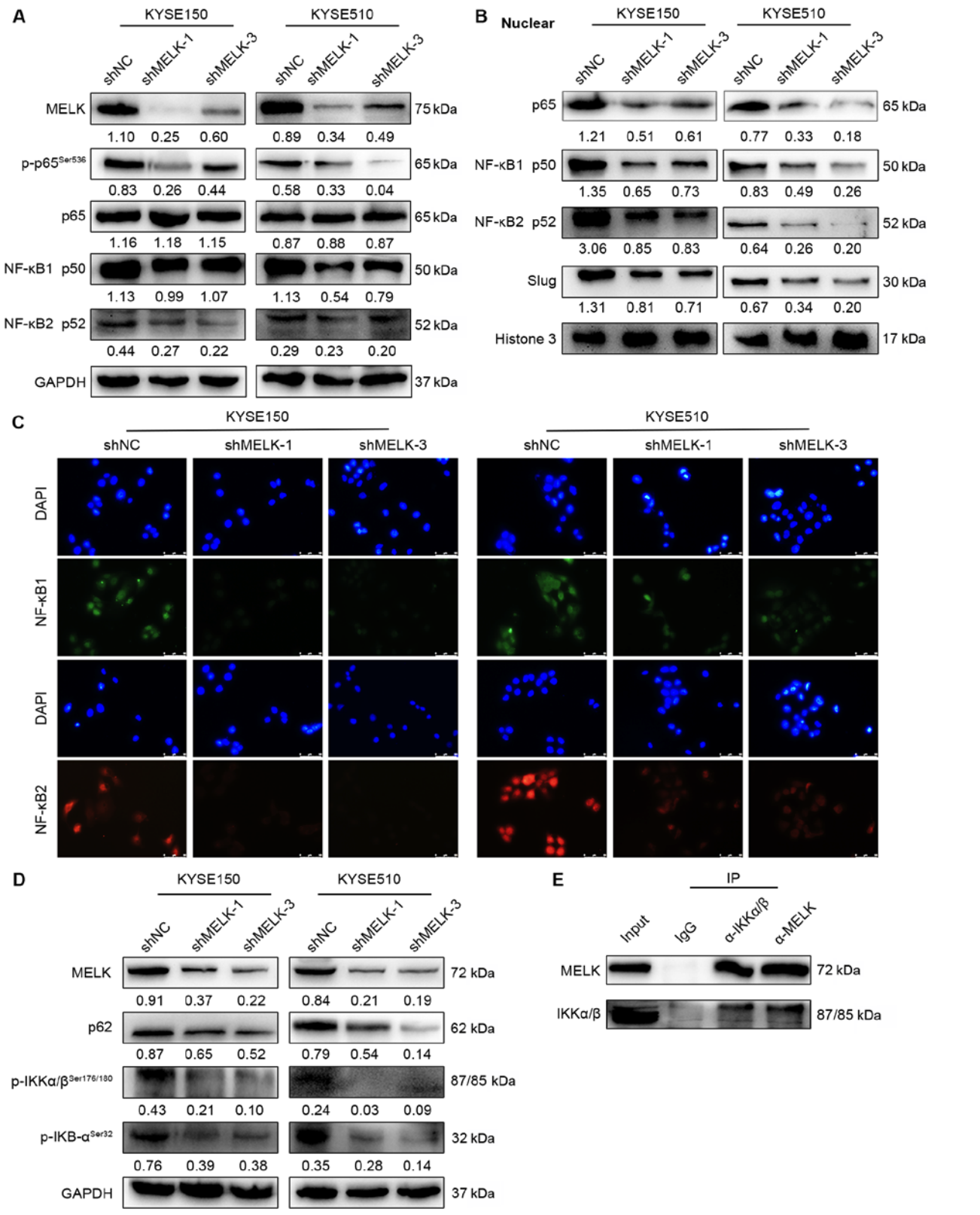

Figure 5. MELK promotes migration and invasion abilities of ESCC cells by activating the NF-κB pathway. (A-D) Western blot analysis of NF-κB pathway-associated proteins in ESCC cells with MELK knockdown. (B) Western blot analysis of NF-κB pathway-associated proteins in the nucleus of ESCC cells with MELK knockdown. (C) Immunofluorescence staining of NF-κB pathway-associated proteins in ESCC cells. Scale bars, 50 μm. (E) Co-immunoprecipitation assays were performed using either MELK or, as a control, IgG antibodies. Data are presented as the mean ± SD of 3 independent experiments. MELK, maternal embryonic leucine zipper kinase; ESCC, esophageal squamous cell carcinoma; NF-κB, nuclear factor-κB; sh, short hairpin RNA; NC, negative control.

induced EMT and promoted cell migration and invasion via the NF-κB pathway (Fig. 8D).

ESCC is one of the most common malignant tumors, and the vast majority of tumor-related deaths are the result of tumor

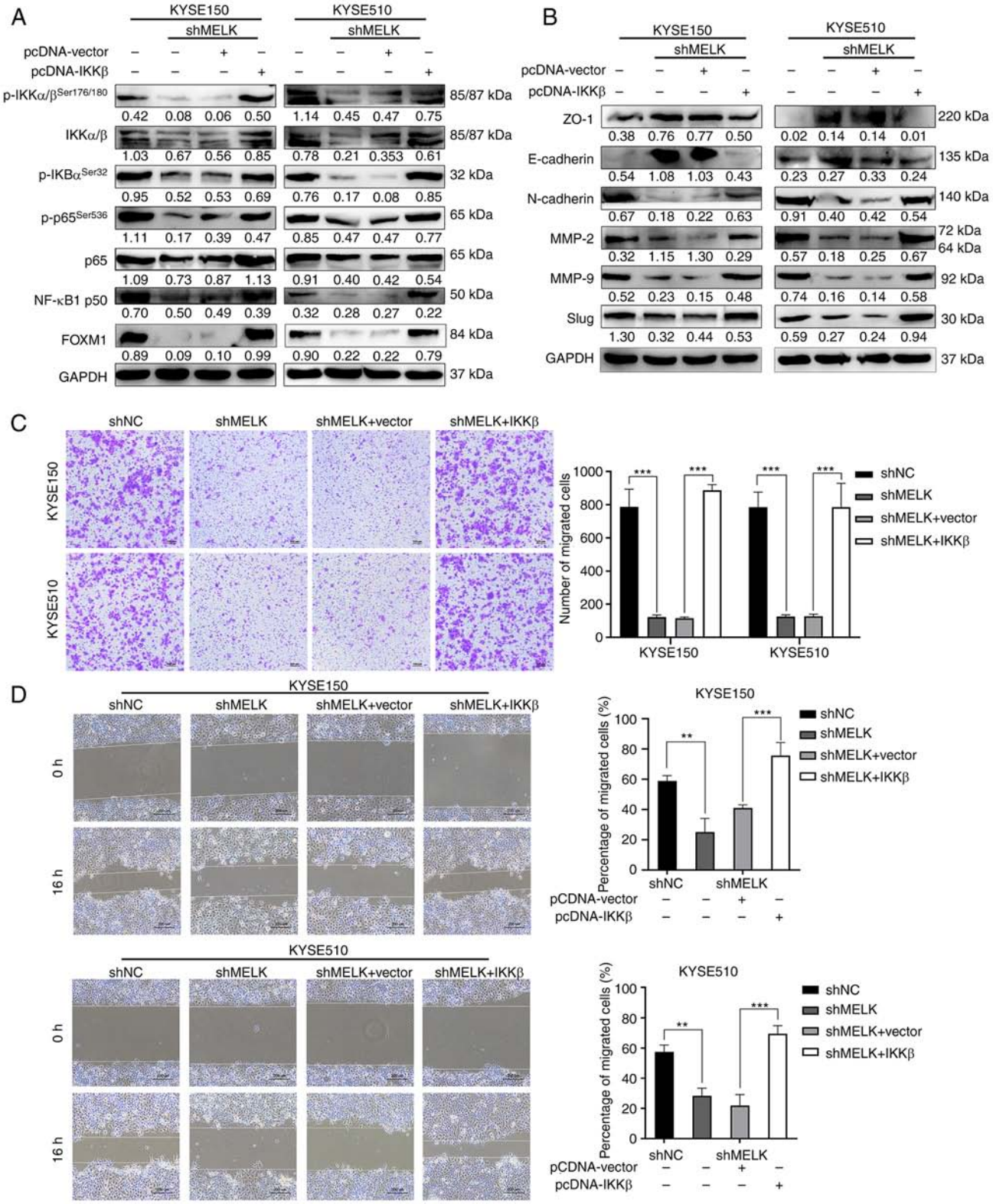

Figure 6. Overexpression of IKKβ rescues the migration ability of MELK-depleted ESCC cell lines. (A) Western blot analysis of NF-κB pathway-associated proteins in ESCC cells with IKKβ overexpression. (B) Western blot analysis of EMT-associated proteins in ESCC cells with IKKβ overexpression. (C) Representative Transwell migration images and statistical analysis of the number of migrated ESCC cells. Scale bars, 100 μm. (D) Representative wound healing assays of migration images and statistical analysis of the percentage of migrated ESCC cells. Scale bars, 200 μm. Data are presented as the mean ± SD of 3 independent experiments. **P<0.01 and ***P<0.001. IKKβ, inhibitor of nuclear factor-κB kinase subunit β; MELK, maternal embryonic leucine zipper kinase; ESCC, esophageal squamous cell carcinoma; NF-κB, nuclear factor-κB; sh, short hairpin RNA; NC, negative control.

metastasis, but the precise molecular mechanisms that drive this metastasis process are largely unknown. Therefore, it is important to understand the molecular events governing tumor proliferation and metastasis to develop novel therapeutic targets in ESCC. Numerous studies have shown that MELK is highly expressed in several tumors, and its expression is correlated

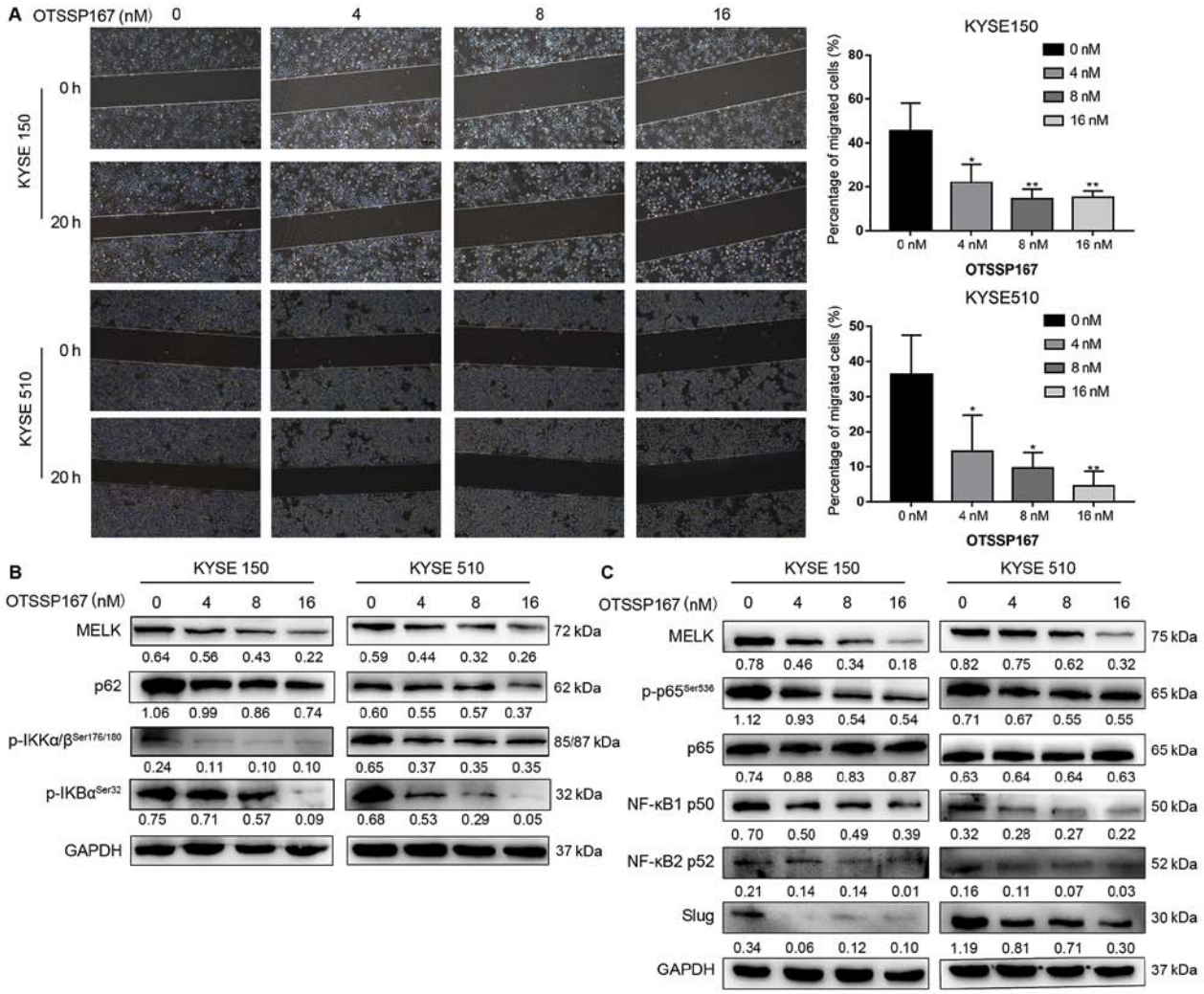

Figure 7. OTSSP167 reduces the migration abilities of ESCC cells by inhibiting the NF-κB pathway. (A) Wound healing assays of the migration of ESCC cells treated with OTSSP167 for 32 h. Scale bars, 100 μm. (B and C) Western blot analysis of NF-κB pathway-associated proteins in ESCC cells treated with OTSSP167 for 24 h. Data are presented as the mean ± SD of 3 independent experiments. *P<0.05 and **P<0.01. ESCC, esophageal squamous cell carcinoma; NF-κB, nuclear factor-κB; MELK, maternal embryonic leucine zipper kinase.

with tumor grade and prognosis (42,43). In the present study, the results showed that MELK expression was significantly upregulated in ESCC compared with normal esophagus epithelium, which is consistent with previous studies in other types of tumors (16,21). Survival analysis revealed that high MELK expression predicted a poor prognosis in patients with ESCC. To further confirm the findings, large sample data from TCGA and GEO databases confirmed the results of MELK expression in the tissue samples of the present study. It was also revealed that positive MELK expression was significantly associated with males. In a previous study, Oliva *et al* revealed that the effects of sex on gene expression are ubiquitous (13,294 sex-biased genes across all tissues) (44). They also discovered that promoters of sex-biased genes are enriched for hormone-related and other transcription factor binding sites (TFBSs) (44). The strongest difference between male- and female-biased enrichment profiles was observed for TFBSs of SP2, SP4, NFYB, TWIST1, and STAT5B (female-biased) and of HNF4G, NFKB1, E2F6, HNF4A, and ETS1 (male-biased), respectively (44). The potential transcription factor of MELK was also analyzed using UCSC Genome Browser, and it was found that HNF4G, E2F6 and HNF4A are the potential transcription factors of MELK. Thus, MELK may be transcriptionally regulated by HNF4G, E2F6 and HNF4A, and function as a male-biased gene. However, this hypothesis warrants further demonstration.

As a serine/threonine protein kinase, MELK was reported to regulate the cell cycle, stem cell renewal, and apoptosis (21,45,46). MELK was also identified to contribute to tumor metastasis and recurrence in breast and gastric cancers (11,47). In the present study, a series of assays were employed to investigate the role of MELK in regulating the characteristic aggressive phenotype of MELK. Knockdown of the expression of MELK ESCC cells *in vitro* was established due to the high expression in ESCC cell lines, and the cell growth, colony formation, and invasion of these cells were investigated. Most previous studies on the function of MELK in tumors have focused on cell growth and apoptosis. The results of the present study suggested that MELK inhibition decreased cell proliferation and colony formation in ESCC cells, consistent with previous studies (16,22,48). However, the cell cycle and apoptosis were not found to be significantly

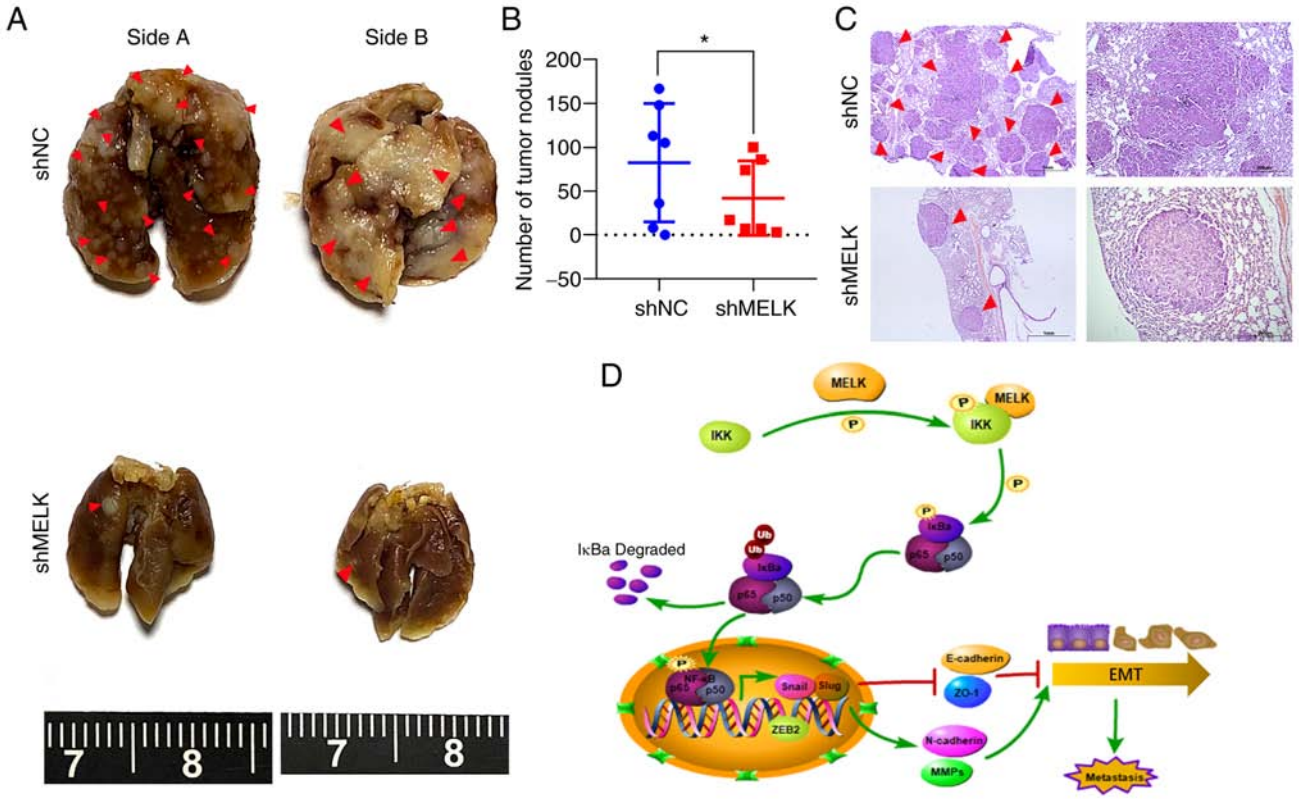

Figure 8. Knockdown of MELK inhibits the metastasis of ESCC cells *in vivo*. (A) KYSE150 cells with MELK knockdown were intravenously injected into nude mice (n=7 per group) through the tail vein. Representative images of excised lungs after 5 weeks of injection are shown (arrows indicate the metastatic foci). (B) The number of tumor nodules on lung surfaces. (C) Lung metastases in each mouse were stained with H&E. Arrows indicate the metastatic colonization of tumor cells in the lung tissues. Scale bars, 1 mm (left), 200 μm (right). (D) Schematic illustrating the role of MELK in stimulating metastasis of ESCC cells. *P<0.05. MELK, maternal embryonic leucine zipper kinase; ESCC, esophageal squamous cell carcinoma; H&E, hematoxylin and eosin; sh, short hairpin RNA; NC, negative control; IKK, IκB kinase; NF-κB, nuclear factor-κB; ZEB2, zinc finger E-box-binding homeobox 2; E-cadherin, epithelial cadherin; ZO-1, zonula occludens-1; N-caherin, neural cadherin; MMPs, matrix metalloproteinases; EMT, epithelial-mesenchymal transition.

influenced by MELK inhibition in ESCC cells. Of note, the cell migration and invasion abilities were inhibited in MELK-knockdown ESCC cells. The metastasis of ESCC cells was also reduced by MELK inhibition *in vivo*. Collectively, the results demonstrated that MELK is an important oncogenic factor and plays critical roles in the cell growth and metastasis of ESCC.

The migration and invasion of cancer cells involve multiple changes in tumor cells (49). EMT is considered one of the major mechanisms involved in solid tumor metastasis (25). It has been reported that EMT progression is accompanied by several crucial changes of epithelial cells, including loss of epithelial adherence, tight junction proteins, loss of cell polarity, and acquisition of a mesenchymal phenotype, leading to invasive and migratory behaviors (7,33). In the present study, the expression levels of EMT-related proteins were examined and it was found that the epithelial markers E-cadherin and ZO-1 were upregulated, while mesenchymal markers N-cadherin, ZEB1, Snail and Slug were downregulated by MELK inhibition in ESCC cells. In addition, MMPs, which are capable of degrading the ECM, were upregulated. Furthermore, GSEA analysis confirmed the association between MELK and aggressive characteristics in ESCC. Collectively, these results revealed that MELK is an important factor for the support of EMT and aggressiveness in ESCC cells.

To date, the precise molecular mechanisms of MELK that promote ESCC cell EMT and aggressive potential remain unknown. MELK reportedly regulates tumor progression by several signaling pathways (16,50,51). The NF-κB pathway is a major tumor-promoting and EMT-related pathway (36,52). A previous study showed that MELK regulates the NF-κB pathway by phosphorylating SQSTM1/p62 and promoting melanoma growth (12). The results of the present study revealed that MELK inhibition decreased the expression of NF-κB transcriptional targets, and reduced translocation to the nucleus of p65, p50, and p52. The expression of p62 was also decreased in MELK-knockdown cells, which was consistent with a previous study (12). The activation of the NF-κB complex relies on the IκB protein being phosphorylated by the IKK complex, which leads to IκB ubiquitination and subsequent degradation (27). In the present study it was determined that the phosphorylation of IκB and IKK were decreased in MELK-knockdown ESCC cells. The findings of the present study were also confirmed by treatment of ESCC cells with the MELK inhibitor OTSSP167 (21,22,40). In addition, co-immunoprecipitation experiments showed that MELK interacted with IKK. The inhibitory effect of MELK knockdown on migration ability and NF-κB signaling could be markedly rescued by overexpression of IKKβ. Therefore, it is proposed that MELK activates the NF-κB pathway by phosphorylating IKKβ. It was determined that MELK interacts with IKK, upstream of IκB, and regulates the expression of p-IκB.

Although MELK may interact with p-IκB, it is considered that the interaction between MELK and IKK is more critical for its molecular function. A previous study claimed that MELK enhanced tumorigenesis, migration, invasion and metastasis of ESCC cells via activation of FOXM1 signaling pathway (23). FOXM1 promoter region contains a functional NF-κB element and is transcriptionally activated upon NF-κB binding in chronic myelogenous leukemia cells (53). There are also FOX binding motifs within the FOXM1 promoter, whose activity is markedly induced after overexpression of p65 (38). In the present study, ectopic expression of IKKβ markedly rescued FOXM1 expression in MELK-silenced ESCC cells, which indicated that FOXM1 is a downstream effector of IKKβ function. Collectively, these results identified MELK as a regulator of the NF-κB pathway and demonstrated that MELK at least partly promotes ESCC metastasis by activating this pathway.

In summary, the results of the present study revealed that MELK regulated the activation of the NF-κB pathway via its inhibitor IKK. In addition, MELK promoted tumor metastasis of ESCC and predicted a poor prognosis in patients with ESCC. Therefore, MELK may be a potential focus of future therapeutic options for ESCC.

Acknowledgements

Not applicable.

Funding

The present study was supported by the Natural Science Foundation of Guangdong Province (grant nos. 2017A030313117 and 2018A030313301), the Guangzhou Science Technology and Innovation Commission (grant no. 201804010075), and the China Postdoctoral Science Foundation (grant no. 2019M663304).

Availability of data and materials

The datasets used and/or analyzed during the current study are available from the corresponding author on reasonable request.

Authors' contributions

LW and XZ conceived and designed the study. JY, WD, YZ, HL, BG, ZQ and PL performed the experiments and acquired the data. JY and WD performed data analysis and drafted the manuscript. JY and LW revised the manuscript for important intellectual content. JY and WD confirmed the authenticity of all the raw data. All authors read and approved the manuscript and agree to be accountable for all aspects of the research in ensuring that the accuracy or integrity of any part of the work are appropriately investigated and resolved.

Ethics approval and consent to participate

All patients and healthy donors signed the written informed consents. The collection and use of tissue samples were approved by the Ethics Committee of the Meizhou People's Hospital (Meizhou, China). The animal experiments were reviewed and approved by the Animal Care and Experimental Committee of Jinan University (approval no. IACUC-20190211-04; Guangzhou, China).

Patient consent for publication

Not applicable.

Competing interests

The authors declare that they have no competing interests.

References

1. Sung H, Ferlay J, Siegel RL, Laversanne M, Soerjomataram I, Jemal A and Bray F: Global cancer statistics 2020: GLOBOCAN estimates of incidence and mortality worldwide for 36 cancers in 185 countries. CA Cancer J Clin 71: 209-249, 2021.
2. Chen MF, Yang YH, Lai CH, Chen PC and Chen WC: Outcome of patients with esophageal cancer: A nationwide analysis. Ann Surg Oncol 20: 3023-3030, 2013.
3. Zeng H, Zheng R, Guo Y, Zhang S, Zou X, Wang N, Zhang L, Tang J, Chen J, Wei K, *et al*: Cancer survival in China, 2003-2005: A population- based study. Int J Cancer 136: 1921-1930, 2015.
4. Zeng H, Chen W, Zheng R, Zhang S, Ji JS, Zou X, Xia C, Sun K, Yang Z, Li H, *et al*: Changing cancer survival in China during 2003-15: A pooled analysis of 17 population-based cancer registries. Lancet Glob Health 6: e555-e567, 2018.
5. Pennathur A, Farkas A, Krasinskas AM, Ferson PF, Gooding WE, Gibson MK, Schuchert MJ, Landreneau RJ and Luketich JD: Esophagectomy for T1 esophageal cancer: Outcomes in 100 patients and implications for endoscopic therapy. Ann Thorac Surg 87: 1048-1054, 2009.
6. Rustgi A and El-Serag HB: Esophageal carcinoma. N Engl J Med 372: 1472-1473, 2015.
7. Diepenbruck M and Christofori G: Epithelial-mesenchymal transition (EMT) and metastasis: Yes, no, maybe? Curr Opin Cell Biol 43: 7-13, 2016.
8. Heyer BS, Warsowe J, Solter D, Knowles BB and Ackerman SL: New member of the Snf1/AMPK kinase family, Melk, is expressed in the mouse egg and preimplantation embryo. Mol Reprod Dev 47: 148-156, 1997.
9. Nakano I, Paucar AA, Bajpai R, Dougherty JD, Zewail A, Kelly TK, Kim KJ, Ou J, Groszer M, Imura T, *et al*: Maternal embryonic leucine zipper kinase (MELK) regulates multipotent neural progenitor proliferation. J Cell Biol 170: 413-427, 2005.
10. Wang Y, Begley M, Li Q, Huang HT, Lako A, Eck MJ, Gray NS, Mitchison TJ, Cantley LC and Zhao JJ: Mitotic MELK-eIF4B signaling controls protein synthesis and tumor cell survival. Proc Natl Acad Sci USA 113: 9810-9815, 2016.
11. Du T, Qu Y, Li J, Li H, Su L, Zhou Q, Yan M, Li C, Zhu Z and Liu B: Maternal embryonic leucine zipper kinase enhances gastric cancer progression via the FAK/Paxillin pathway. Mol Cancer 13: 100, 2014.
12. Janostiak R, Rauniyar N, Lam TT, Ou J, Zhu LJ, Green MR and Wajapeyee N: MELK promotes melanoma growth by stimulating the NF-κB pathway. Cell Rep 21: 2829-2841, 2017.
13. Wang Y, Lee YM, Baitsch L, Huang A, Xiang Y, Tong H, Lako A, Von T, Choi C, Lim E, *et al*: MELK is an oncogenic kinase essential for mitotic progression in basal-like breast cancer cells. Elife 3: e01763, 2014.
14. Kuner R, Falth M, Pressinotti NC, Brase JC, Puig SB, Metzger J, Gade S, Schäfer G, Bartsch G, Steiner E, *et al*: The maternal embryonic leucine zipper kinase (MELK) is upregulated in high-grade prostate cancer. J Mol Med (Berl) 91: 237-248, 2013.
15. Kig C, Beullens M, Beke L, Van Eynde A, Linders JT, Brehmer D and Bollen M: Maternal embryonic leucine zipper kinase (MELK) reduces replication stress in glioblastoma cells. J Biol Chem 292: 12786, 2017.
16. Xu Q, Ge Q, Zhou Y, Yang B, Yang Q, Jiang S, Jiang R, Ai Z, Zhang Z and Teng Y: MELK promotes endometrial carcinoma progression via activating mTOR signaling pathway. EBioMedicine 51: 102609, 2020.
17. Pitner MK, Taliaferro JM, Dalby KN and Bartholomeusz C: MELK: A potential novel therapeutic target for TNBC and other aggressive malignancies. Expert Opin Ther Targets 21: 849-859, 2017.

18. Guan S, Lu J, Zhao Y, Yu Y, Li H, Chen Z, Shi Z, Liang H, Wang M, Guo K, *et al*: MELK is a novel therapeutic target in high-risk neuroblastoma. Oncotarget 9: 2591-2602, 2018.
19. Ikeda Y, Sato S, Yabuno A, Shintani D, Ogasawara A, Miwa M, Zewde M, Miyamoto T, Fujiwara K, Nakamura Y and Hasegawa K: High expression of maternal embryonic leucine-zipper kinase (MELK) impacts clinical outcomes in patients with ovarian cancer and its inhibition suppresses ovarian cancer cells growth ex vivo. J Gynecol Oncol 31: e93, 2020.
20. Liu H, Sun Q, Sun Y, Zhang J, Yuan H, Pang S, Qi X, Wang H, Zhang M, Zhang H, *et al*: MELK and EZH2 cooperate to regulate medulloblastoma cancer stem-like cell proliferation and differentiation. Mol Cancer Res 15: 1275-1286, 2017.
21. Chen S, Zhou Q, Guo Z, Wang Y, Wang L, Liu X, Lu M, Ju L, Xiao Y and Wang X: Inhibition of MELK produces potential anti-tumour effects in bladder cancer by inducing G1/S cell cycle arrest via the ATM/CHK2/p53 pathway. J Cell Mol Med 24: 1804-1821, 2020.
22. Kohler RS, Kettelhack H, Knipprath-Meszaros AM, Fedier A, Schoetzau A, Jacob F and Heinzelmann-Schwarz V: MELK expression in ovarian cancer correlates with poor outcome and its inhibition by OTSSP167 abrogates proliferation and viability of ovarian cancer cells. Gynecol Oncol 145: 159-166, 2017.
23. Chen L, Wei Q, Bi S and Xie S: Maternal embryonic leucine zipper kinase promotes tumor growth and metastasis via stimulating FOXM1 signaling in esophageal squamous cell carcinoma. Front Oncol 10: 10, 2020.
24. Dongre A and Weinberg RA: New insights into the mechanisms of epithelial-mesenchymal transition and implications for cancer. Nat Rev Mol Cell Biol 20: 69-84, 2019.
25. Pastushenko I and Blanpain C: EMT transition states during tumor progression and metastasis. Trends Cell Biol 29: 212-226, 2019.
26. Yamini B: NF-κB, mesenchymal differentiation and glioblastoma. Cells 7: 125, 2018.
27. Zhang Q, Lenardo MJ and Baltimore D: 30 years of NF-κB: A blossoming of relevance to human pathobiology. Cell 168: 37-57, 2017.
28. Greene FL, Page DL, Fleming ID, Fritz AG, Balch CM, Haller DG and Morrow M (eds). Esophagus. In: AJCC cancer staging manual. Springer, New York, NY, pp91-98, 2002.
29. Livak KJ and Schmittgen TD: Analysis of relative gene expression data using real-time quantitative PCR and the 2(-Delta Delta C(T)) method. Methods 25: 402-408, 2001.
30. Hu N, Clifford RJ, Yang HH, Wang C, Goldstein AM, Ding T, Taylor PR and Lee MP: Genome wide analysis of DNA copy number neutral loss of heterozygosity (CNNLOH) and its relation to gene expression in esophageal squamous cell carcinoma. BMC Genomics 11: 576, 2010.
31. Su H, Hu N, Yang HH, Wang C, Takikita M, Wang QH, Giffen C, Clifford R, Hewitt SM, Shou JZ, *et al*: Global gene expression profiling and validation in esophageal squamous cell carcinoma and its association with clinical phenotypes. Clin Cancer Res 17: 2955-2966, 2011.
32. Rickman DS, Millon R, De Reynies A, Thomas E, Wasylyk C, Muller D, Abecassis J and Wasylyk B: Prediction of future metastasis and molecular characterization of head and neck squamous-cell carcinoma based on transcriptome and genome analysis by microarrays. Oncogene 27: 6607-6622, 2008.
33. Sarrio D, Rodriguez-Pinilla SM, Hardisson D, Cano A, Moreno-Bueno G and Palacios J: Epithelial-mesenchymal transition in breast cancer relates to the basal-like phenotype. Cancer Res 68: 989-997, 2008.
34. Liberzon A, Birger C, Thorvaldsdottir H, Ghandi M, Mesirov JP and Tamayo P: The molecular signatures database (MSigDB) hallmark gene set collection. Cell Syst 1: 417-425, 2015.
35. Shimada Y, Imamura M, Wagata T, Yamaguchi N and Tobe T: Characterization of 21 newly established esophageal cancer cell lines. Cancer 69: 277-284, 1992.
36. Pires BR, Mencalha AL, Ferreira GM, de Souza WF, Morgado-Díaz JA, Maia AM, Corrêa S and Abdelhay ESF: NF-kappaB is involved in the regulation of EMT genes in breast cancer cells. PLoS One 12: e0169622, 2017.
37. Hoesel B and Schmid JA: The complexity of NF-κB signaling in inflammation and cancer. Mol Cancer 12: 86, 2013.
38. Li Y, Lu L, Tu J, Zhang J, Xiong T, Fan W, Wang J, Li M, Chen Y, Steggerda J, *et al*: Reciprocal regulation between forkhead box M1/NF-κB and methionine adenosyltransferase 1A drives liver cancer. Hepatology 72: 1682-1700, 2020.
39. Zhang Y, Zhou X, Li Y, Xu Y, Lu K, Li P and Wang X: Inhibition of maternal embryonic leucine zipper kinase with OTSSP167 displays potent anti-leukemic effects in chronic lymphocytic leukemia. Oncogene 37: 5520-5533, 2018.
40. Cho YS, Kang Y, Kim K, Cha YJ and Cho HS: The crystal structure of MPK38 in complex with OTSSP167, an orally administrative MELK selective inhibitor. Biochem Biophys Res Commun 447: 7-11, 2014.
41. Li G, Yang M, Zuo L and Wang MX: MELK as a potential target to control cell proliferation in triple-negative breast cancer MDA-MB-231 cells. Oncol Lett 15: 9934-9940, 2018.
42. Li Y, Li Y, Chen Y, Xie Q, Dong N, Gao Y, Deng H, Lu C and Wang S: Correction to: MicroRNA-214-3p inhibits proliferation and cell cycle progression by targeting MELK in hepatocellular carcinoma and correlates cancer prognosis. Cancer Cell Int 18: 55, 2018.
43. Bollu LR, Shepherd J, Zhao D, Ma Y, Tahaney W, Speers C, Mazumdar A, Mills GB and Brown PH: Mutant P53 induces MELK expression by release of wild-type P53-dependent suppression of FOXM1. NPJ Breast Cancer 6: 2, 2020.
44. Oliva M, Munoz-Aguirre M, Kim-Hellmuth S, Wucher V, Gewirtz ADH, Cotter DJ, Parsana P, Kasela S, Balliu B, Viñuela A, *et al*: The impact of sex on gene expression across human tissues. Science 369: eaba3066, 2020.
45. Ren L, Deng B, Saloura V, Park JH and Nakamura Y: MELK inhibition targets cancer stem cells through downregulation of SOX2 expression in head and neck cancer cells. Oncol Rep 41: 2540-2548, 2019.
46. Wang K, Zhu X, Yao Y, Yang M, Zhou F and Zhu L: Corosolic acid induces cell cycle arrest and cell apoptosis in human retinoblastoma Y-79 cells via disruption of MELK-FoxM1 signaling. Oncol Rep 39: 2777-2786, 2018.
47. Speers C, Zhao SG, Kothari V, Santola A, Liu M, Wilder-Romans K, Evans J, Batra N, Bartelink H, Hayes DF, *et al*: Maternal embryonic leucine zipper kinase (MELK) as a novel mediator and biomarker of radioresistance in human breast cancer. Clin Cancer Res 22: 5864-5875, 2016.
48. Tian JH, Mu LJ, Wang MY, Zeng J, Long QZ, Guan B, Wang W, Jiang YM, Bai XJ and Du YF: BUB1B promotes proliferation of prostate cancer via transcriptional regulation of MELK. Anticancer Agents Med Chem 20: 1140-1146, 2020.
49. Mierke CT: The matrix environmental and cell mechanical properties regulate cell migration and contribute to the invasive phenotype of cancer cells. Rep Prog Phys 82: 064602, 2019.
50. Seong HA, Manoharan R and Ha H: Zinc finger protein ZPR9 functions as an activator of AMPK-related serine/threonine kinase MPK38/MELK involved in ASK1/TGF-beta/p53 signaling pathways. Sci Rep 7: 42502, 2017.
51. Gu C, Banasavadi-Siddegowda YK, Joshi K, Nakamura Y, Kurt H, Gupta S and Nakano I: Tumor-specific activation of the C-JUN/MELK pathway regulates glioma stem cell growth in a p53-dependent manner. Stem Cells 31: 870-881, 2013.
52. Ren D, Yang Q, Dai Y, Guo W, Du H, Song L and Peng X: Oncogenic miR-210-3p promotes prostate cancer cell EMT and bone metastasis via NF-κB signaling pathway. Mol Cancer 16: 117, 2017.
53. Jin B, Wang C, Li J, Du X, Ding K and Pan J: Anthelmintic niclosamide disrupts the interplay of p65 and FOXM1/β-catenin and eradicates leukemia stem cells in chronic myelogenous leukemia. Clin Cancer Res 23: 789-803, 2017.